The composite improved improved Generalized Steinmetz Equation (ci^{2}GSE): Pushing Analytical Models to the Limit

Asier Arruti, Borja Alberdi, Anartz Agote, Iosu Aizpuru

Abstract- This document presents a compact core loss model designed to be presented in magnetic material datasheets built upon well known works regarding the topic, while adhering to the MagNet challenge evaluation criteria. The inputs have been modified to better fit a typical magnetic device design workflow, where the flux waveforms are typically simplified versions. Then the developed model is presented, which is built upon the basis of loss separation into hysteresis and eddy losses, composite waveform hypothesis, and relaxation losses. All these effects are modelled in a small number of parameters, 3 for the hysteresis losses, 3 for the eddy losses and 3 for the relaxation losses. Lastly the obtained results are presented, followed by a discussion on why we believe this model is an excellent candidate for magnetic material datasheets.

Index Terms- Core loss modelling, MagNet challenge.

I. Introduction

The following document represents the MagNet challenge final report presented by the Mondragon University team.

Our objective in the MagNet challenge was to generate a model that is simple enough to be presented in magnetic material datasheets while following the MagNet challenge evaluation criteria:

- Model accuracy (30%): although in the MagNet challenge the 95th percentile is the criteria to evaluate, we decided to focus in minimizing the root mean square error instead, since we believe that the 95th percentile goes against the concept of generalizable models, which should be the key criteria in the generation of a standard material loss definition.
- Model size (30%): the model should be as compact as possible, making a significant trade of accuracy vs size if this means that the model can be defined in a small number of parameters ideal for publishing in the material datasheets along loss curves.
- Model explainability (20%): the model is based on well known analytical approaches for loss calculation (hysteresis loss, eddy loss and relaxation loss), [1]-[4], facilitating its adoption in industry and combination with other works based on the Steinmetz Equations (like the Steinmetz Premagnetization Graph [5]).
- Model novelty (10%): model size and accuracy have the same weight in the evaluation criteria (30% and 30%), but we believe that most teams will focus on the accuracy part, while our approach will focus in generating a compact and generalizable model that can be easily presented in material datasheets.
- Software quality (10%): the model should be easy to understand an implement in different environments (even in basic tools such as EXCEL).

As the title suggest, the proposed model is based on analytical models, mainly using 4 main pillars:

I. True Steinmetz Equation (tSE): assumption that two terms are necessary to accurately define the core loss behavior at low (hysteresis losses) and high (eddy losses) frequencies [1].

II. The improved generalized Steinmetz Equation (iGSE): assumption that the losses of non-sinusoidal waveforms can be defined using the flux derivative (dB/dt) and peak to peak flux density (ΔB) of the waveform [2].

III. The composite waveform hypothesis (CWH): assumption that in triangular/trapezoidal flux waveforms the losses of each segment can be calculated separately [3].

IV. The improved improved generalized Steinmetz Equation (i^{2}GSE): assumption that trapezoidal waveform with zero voltage segments increase the total losses due to relaxation effect [4].

The composite improved improved Generalized Steinmetz Equation (ci2GSE) presented in this work is the natural continuation of the composite improved Generalized Steinmetz Equation (ciGSE) model first conceptualized in [6]. The ciGSE was created as an accurate alternative to the iGSE for high and low duty cycle triangular waveforms, combining the CWH and iGSE in a way that allows to retain the direct connection with the Steinmetz Parameters. The preliminary report sent on the 10th of November details the limitations of the ciGSE found during the MagNet challenge, which have been completely solved in this iteration of the model:

I. The characterization of the loss model is fully automated and 100% generalizable between materials and temperatures. The automatic parametrization can predict the optimal parameters from the same initial points for all materials.

II. The extrapolation problem has been completely solved with the use of the dual loss plane based on the tSE, where two planes are used to define the low frequency (hysteresis) and high frequency (eddy) losses. This also

Asier Arruti, Borja Alberdi, Anar Agote and Iosu Aizpuru are with the Faculty of Engineering, Mondragon University, Mondragon, Spain (e-mail: aarruti@mondragon.edu; janzola@mondragon.edu; iaizpuru@mondragon.edu; mmazuela@mondragon.edu).

reduces the amount of parameters necessary substantially, but entails a loss in accuracy in the low to high frequency transition. Still, the final accuracies are still impressive for the very compact model achieved, which is in accordance with our defined criteria.

The following report will describe the presented model in various sections. First, in Section II the necessary changes of the input data to use the model will be described. Then, in Section III the main model is presented, with the necessary steps to parametrize the model and representation of the different physical phenomena governing core losses. Then, on Section IV the results achieved with the model for the preliminary 10 materials and the final 5 materials are presented. Lastly, a discussion about the model is presented in Section V followed by the conclusions in Section VI.

II. Input Data Structure

Since the ciGSE was initially developed to be used in the design process of transformers for core loss estimations, the inputs disagree with the ones presented by the MagNet challenge and resemble more the simplified waveforms segments typically used in classical approaches such as the iGSE. The MagNet challenge present experimental flux waveforms, while in the design process these are not available.

Thus, the flux waveforms must be transformed into basic segments, requiring a preprocessing of the data. The algorithm proposed to do so first classifies the flux waveforms into three categories:

I. Sinusoidal waveforms: the fast Fourier transform is applied to the flux waveform, and if the main harmonic is much higher than the rest the waveform is classified as sinusoidal.
II. Triangular waveforms: the derivatives of the flux waveforms are obtained and if they have only two levels, the waveform is classified as triangular. The duty cycles are obtained from the derivative of the flux density.
III. Trapezoidal waveforms: same approach as triangular waveforms but if three levels are detected the waveform is trapezoidal. The duty cycles are also obtained from the derivative of the flux density.

Note that this classification is not perfect, and sometimes can result in wrong classification of the waveform. Also, the duty cycles are defined in a resolution of 0.1, which appears to be the resolution used in the MagNet database.

After the classification, simplified waveforms based on segments are generated to use with the proposed model. Examples of these simplified waveforms are shown in Fig. 1, a trapezoidal waveform with relaxation, a trapezoidal waveform without relaxation, and a triangular waveform. It is clear that these waveforms are not exactly the same as the non simplified flux waveforms, but are more akin to typical waveforms found in the design process of magnetic devices.

The necessary parameters to define these simplified waveforms then become:

Sinusoidal	Frequency	[Nx1]
	Peak to Peak Flux	[Nx1]
Triangular	Frequency	[Nx1]
	Duty cycle	[Nx2]
	Flux change	[Nx2]
	Flux derivative	[Nx2]
Trapezoidal	Frequency	[Nx1]
	Duty cycle	[Nx4]
	Flux change	[Nx4]
	Flux derivative	[Nx4]

where N is the number of waveforms.

REMARK: This initial preprocessing algorithm is a very simple approach, and will work in most cases, but from the initial 10 materials it has been seen that it sometimes fails in the classification of 1% to 2% of the waveforms. This would not be too much of a problem if the models are optimized for the 95th percentile, but since we decided to use the root mean square error, this data classification problem has an impact in the overall results. It should also be noted that at high frequencies the transition of the flux density derivative is not instant and using the 0.1 duty cycle resolution results in the simplified waveform not completely resembling the original waveform. Unfortunately, optimizing this algorithm would take too much time and effort away form the development of the main model, since the only way to correctly verify this would be to one by one plot the original and simplified waveforms and check for discrepancies.

III. The ci^{2}GSE Model

As mentioned in the introduction, the proposed ci^{2}GSE is based on 4 critical pillars from existing literature of analytical modelling of core losses.

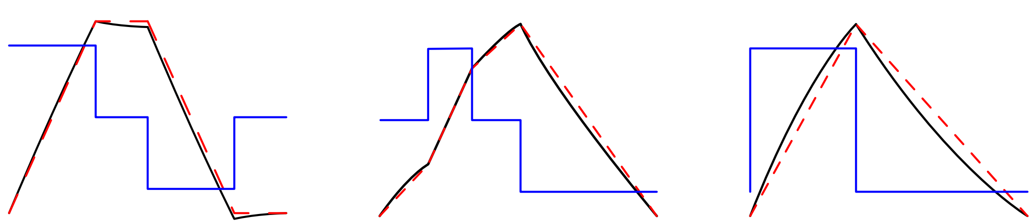

Fig. 1: Examples of two trapezoidal and triangular waveforms transformed in their equivalent simplified waveforms. Original flux waveform (**black**), flux derivative (**blue**) and reconstructed simplified waveform (**red**).

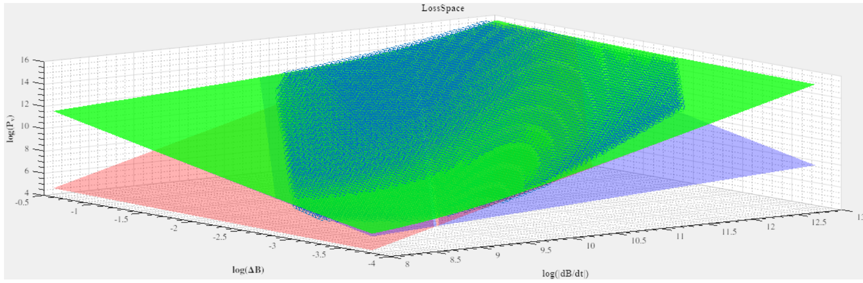

Fig. 2: Losses of each waveform segments as functions of flux density derivative and peak to peak flux density. Here the low frequency hysteresis losses (blue plane) and high frequency eddy losses (red plane) can be clearly visualized.

Beginning from the first one, the true Steinmetz Equation (tSE) which is the original Steinmetz equation presented in [5] to model the core losses, looks like this:

$$P_{\text{loss}} = k_1 f B^{b_1} + k_2 f^2 B^2 \tag{1}$$

Here, the first part refers to the hysteresis losses and the second term to the high frequency eddy losses. This can be rewritten in a similar manner to the iGSE, so it is defined as functions of the flux derivative dB/dt and peak to peak flux density ΔB:

$$P_{\text{loss}} = \frac{1}{\mathrm{T}}\int_0^T \left[k_1 \left|\frac{dB}{dt}\right|^{a_1} \Delta B^{b_1} + k_2 \left|\frac{dB}{dt}\right|^{a_2} \Delta B^{b_2}\right] \tag{2}$$

The introduction of the two adding terms in the core loss definition is critical to represent the influence of the non-constant Steinmetz Parameters, meaning that unlike in the iGSE, if we have two segments with very different dB/dt values, the impact of the low frequency hysteresis losses and high frequency eddy losses are modeled independently in each segment. This is how the findings from the CWH [3] can be considered in our model, allowing to estimate the losses of high and low duty cycle waveforms much more accurately than the classical iGSE approach. This same concept was reported in our previous publication of the ciGSE [6].

Now, in our previous work [6] we used fifth degree polynomial surfaces (where X Y Z are the logarithmic values of dB/dt, ΔB and P_{loss} respectively) to model the losses in each segment, but although this results in very accurate estimations, it generates problems when extrapolation is used. The new proposed model (2) is less accurate but can define the losses with only 6 parameters and should mathematically be able to semi-accurately predict the losses at ultra-low and ultra-high frequencies as shown in our preliminary report.

The task in hand becomes in how to use the MagNet data to obtain the necessary parameters k_1, a_1, b_1, k_2, a_2 and b_2. What we propose in our model is to use all triangular data and trapezoidal data without relaxation effect to fit these parameters minimizing the total root mean square error. To do so we found that rewritten (2) into the following form helps the fitting algorithm find the optimal parameters,

$$\begin{aligned} P_{\text{loss}} = \sum D \Big[&\exp\left(k_1' + a_1 \ln\left|\tfrac{dB}{dt}\right| + b_1 \ln \Delta B\right) \\ &+ \exp\left(k_2' + a_2 \ln\left|\frac{dB}{dt}\right| + b_2 \ln \Delta B\right)\Big] \end{aligned} \tag{3}$$

where D is the duty cycle, and the summation term represented the addition of the losses of all segments. Note that the ΔB term is not the flux density change in a segment, but the peak to peak flux density in the waveform, as defined according to the iGSE in [2].

The idea behind this concept is that the core losses are generally quite linear in logarithmic dimensions, thus using k', a and b the loss space is a combination of two planes. This is better visualized in Fig. 2 where the core losses (per segment) in logarithmic dimensions are shown to fit two planes. The blue plane represents the low frequency losses (hysteresis losses) while the red plane represents the high frequency losses (eddy losses). The green plane is the combination of both planes, fitting the MagNet data quire closely.

From physical understanding of the hysteresis and eddy losses, we can make some approximations of the initial k_1', a_1, b_1, k_2', a_2 and b_2 parameters. We know that for the low frequency losses (blue plane) ideally the a_1 parameters should be close to 1 since the hysteresis losses are assumed to increase proportionally with frequency. For the high frequency losses, we have more information, since we know that the eddy losses are a function of the square of dB/dt, thus a_2 should be close to 2 while b_2 should be approximately 0. We can also make estimations of the value of k_2', since this value should relate to the resistivity of the core material, which for ferrites is commonly around 1 to 10 Ωm, meaning k_2 values of 1e^{-6} or 1e^{-7}, or k_2' values around -13.8 and -16.1.

Based on our analysis of the initial 10 materials, we proposed using initial values of k_1' = 5, a_1 = 0.75, b_1 = 1.75, $k_2' = -15$, a_2 = 2 and b_2 = 0. Then, we can let the computer try to minimize the resulting root mean square error from (3) to find the ‘optimal’ values. Different algorithms can be used for this optimization, although we found that the basic MATLAB’s function to find the minimum of an unconstrained multivariable function (`fminunc`) works correctly.

Of course, due to the relaxation effect reported in [4], this approach will not be able to accurately estimate the losses in trapezoidal waveforms like the first one shown on Fig. 1. To solve this issue, a new term must be added to (3) to consider the increased losses. To do so, we first need to quantify the discrepancy in losses due to relaxation effect, which we can do by comparing the estimated losses using (3) and the real measured losses from the MagNet data. From here we can define the relaxation energy:

$$E_{rel} = \frac{\left(P_{real} - P_{pred}\right)}{f} \tag{4}$$

where P_{real} are the losses given in the MagNet data and P_{pred} are the losses estimated using (3). Once the relaxation energies E_{rel} are obtained, we can try to generate a mathematical definition for these. Although this problem was already tackled in the i^2GSE [4], the equation presented there is not that easy to implement for thousands of waveforms at different frequencies and flux density levels. Based on the assumption that the relaxation losses are governed by mainly two parameters, the flux density ΔB and the relaxation time t_{rel}, we found that

$$E_{rel} = \exp(k'_{rel} + a_{rel}\ln t_{rel} + b_{rel}\ln \Delta B) \tag{5}$$

is in most cases good enough to achieve decent predictions of the increase in core losses. In this case, since (5) also represents a plane in logarithmic space similar to those shown in Fig. 2, the parameters can be extracted easily without requiring to define the initial points. Still, logic dictates that, according to the findings from [4], the a_{rel} parameters should be between 0 and 1 since the relaxation energy increases with the relaxation time (>0) but in a decaying exponential function (<1).

With (3) and (5) we have everything needed to evaluate all trapezoidal and triangular waveforms, but since we have obtained the necessary parameters in two steps, we run into the risk of not finding the globally optimal parameters. Thus, as a last step the parameters should be reoptimized using a combination of (3) and (5):

$$\begin{aligned} P_{\text{loss}} = \sum \Bigg[D \Bigg(&\exp\left(k'_1 + a_1 \ln\left|\frac{dB}{dt}\right| + b_1 \ln \Delta B\right) \\ &+ \exp\left(k'_2 + a_2 \ln\left|\frac{dB}{dt}\right| + b_2 \ln \Delta B\right)\Bigg)\Bigg] \\ &+ f \exp\left(k'_{rel} + a_{rel}\ln t_{rel} + b_{rel} \ln \Delta B\right) \end{aligned} \tag{6}$$

where we can use the already obtained parameters as initial points.

According to our findings this last optimization is capable to reduce the root mean square error by up to x0.70 in some cases. The 95th percentile error usually also decreases by around x0.95 in most cases, but in some situations this last optimization step can increase the 95th percentile by up to x1.05 since we still optimize the parameters for the minimum root mean square error.

Note that until now only triangular and trapezoidal waveforms have been analyzed. For sinusoidal waveforms we opted to simply fit the sinusoidal loss data into a second-degree polynomial plane where X Y Z are the logarithmic values of f, ΔB and P_{loss} respectively. This polynomial plane is then defined with 6 parameters: *p00*, *p10*, *p01*, *p20*, *p11* and *p02*.

In the future we hope to use the well stablished physical connection between the iGSE and classical sinusoidal loss Steinmetz Equation to use the same parameters for sinusoidal, triangular, and trapezoidal waveforms.

IV. Obtained Results

With the model presented, TABLE I presents the fitting parameters and results achieved for the preliminary 10 materials.

TABLE I: RESULTS FOR THE PRELIMINARY 10 MATERIALS

Mat	Temp	k'_1	a_1	b_1	k'_2	a_2	b_2	k'_{rel}	a_{rel}	b_{rel}	E_{95th}
				p00	*p10*	*p01*	*p20*	*p11*	*p02*		
3C90	25ºC	3.2949	0.9926	1.5387	-18.0861	2.5519	-0.1489	9.4304	0.5558	2.2764	
				38.2471	-5.2966	1.7308	0.2886	0.0683	-0.0046		
	50ºC	1.9388	1.1001	1.6632	-18.4833	2.5520	-0.3359	10.8116	0.6566	2.5594	
				54.6290	-8.1188	2.4717	0.4111	0.0358	0.0632		
	70ºC	1.8146	1.1170	1.9345	-17.8307	2.5006	-0.3363	11.6266	0.7022	2.8748	
				74.7656	-11.5452	3.5607	0.5583	-0.0188	0.1438		
	90ºC	0.5324	1.2379	2.0636	-17.8128	2.4918	-0.3789	14.3733	0.9090	3.0760	
				78.5242	-12.1494	4.6619	0.5855	-0.0721	0.2385		
	All	60 parameters, 4x(9+6)									15.87%
3C94	25ºC	3.1540	0.9761	1.4614	-16.0243	2.4074	-0.0485	8.8663	0.5214	2.2247	
				35.0271	-4.7595	1.8163	0.2640	0.0365	-0.0510		
	50ºC	1.7237	1.0830	1.6383	-15.7103	2.3611	-0.1608	9.2033	0.5471	2.5406	
				53.5046	-7.9783	2.8914	0.4037	-0.0251	0.0182		
	70ºC	0.7116	1.1702	1.9055	-14.9323	2.2931	-0.1706	8.6424	0.4904	2.9140	
				50.4689	-7.4381	4.4394	0.3805	-0.1279	0.0901		
	90ºC	-1.7024	1.3837	1.9884	-15.0473	2.2875	-0.2278	9.7426	0.5575	3.2584	
				37.9566	-5.3024	5.4287	0.2912	-0.1815	0.1663		
	All	60 parameters, 4x(9+6)									13.27%
3E6	25ºC	0.0171	1.1847	1.4276	-10.8203	2.0126	-0.0477	8.5535	0.5355	2.0393	
				-4.0702	1.8256	4.2533	-0.0131	-0.1611	0.0307		
	50ºC	1.4756	1.0670	1.4486	-9.0378	1.9104	0.0629	8.3426	0.5284	1.7438	
				-3.9316	1.8870	4.2768	-0.0183	-0.1754	0.0019		
	70ºC	0.9241	1.1102	1.2908	-8.4753	1.8720	0.0795	8.1050	0.5144	1.6260	
				-6.0839	2.2824	4.1452	-0.0360	-0.1693	-0.0043		
	90ºC	-0.3152	1.2309	1.0344	-9.6984	1.9477	-0.0126	7.4695	0.4876	1.4387	
				-7.2634	2.4448	3.6225	-0.0410	-0.1228	0.0122		
	All	60 parameters, 4x(9+6)									6.048%
3F4	25ºC	7.2635	0.7721	2.0404	-11.8211	2.1937	0.7243	10.5991	0.5842	2.2452	
				39.7314	-5.5639	-0.2123	0.3146	0.2895	0.0513		
	50ºC	4.6360	1.0032	1.9359	-21.6308	2.7726	-0.1841	10.3548	0.5705	2.2826	
				41.4321	-5.8034	0.0469	0.3258	0.3069	0.1275		
	70ºC	4.1859	1.0438	1.9569	-24.7371	2.9376	-0.5927	11.1837	0.6283	2.3416	
				35.1985	-4.3968	1.7572	0.2554	0.2110	0.2502		
	90ºC	4.0261	1.0642	1.9695	-24.2859	2.8819	-0.7292	12.0015	0.6747	2.4572	
				37.2316	-4.7229	1.9112	0.2688	0.1996	0.2450		
	All	60 parameters, 4x(9+6)									20.14%
77	25ºC	3.7371	0.9372	1.4237	-16.1308	2.4407	-0.0044	8.5796	0.5016	2.1180	
				27.2048	-3.3242	1.9860	0.1988	0.0003	-0.1050		
	50ºC	1.3287	1.1311	1.4277	-17.3259	2.4909	-0.2305	9.4489	0.5778	2.3135	
				43.8908	-6.2703	2.5613	0.3288	-0.0151	-0.0280		
	70ºC	-0.0006	1.2417	1.6690	-16.7898	2.4360	-0.2945	11.2179	0.7019	2.7183	
				52.6721	-7.7892	3.9760	0.3958	-0.0928	0.0684		
	90ºC	-2.3497	1.4469	1.6627	-17.0067	2.4349	-0.3837	8.8988	0.5056	2.9511	
				41.6649	-5.8257	5.5376	0.3113	-0.1906	0.1451		
	All	60 parameters, 4x(9+6)									14.34%
78	25ºC	3.0371	1.0024	1.4597	-16.8690	2.4838	-0.0916	9.4090	0.5610	2.2070	
				37.0729	-5.0321	2.1191	0.2741	0.0148	-0.0465		
	50ºC	1.2854	1.1428	1.5804	-17.1200	2.4738	-0.2441	10.5646	0.6514	2.4860	
				50.6142	-7.4068	3.0851	0.3787	-0.0307	0.0355		
	70ºC	-0.8585	1.3263	1.7031	-17.2370	2.4621	-0.3446	12.1486	0.7657	2.8140	
				54.6531	-8.1183	4.2803	0.4117	-0.0935	0.1238		
	90ºC	-2.1911	1.4453	1.7032	-17.2121	2.4516	-0.3835	8.1462	0.4389	2.9331	
				46.0493	-6.5545	5.4940	0.3429	-0.1765	0.1643		
	All	60 parameters, 4x(9+6)									15.98%
N27	25ºC	4.3365	0.9017	1.4604	-15.3586	2.3917	0.0633	8.5848	0.4827	2.1194	
				28.8196	-3.6304	1.5094	0.2145	0.0482	-0.0831		
	50ºC	1.9238	1.0985	1.5119	-16.6799	2.4481	-0.1812	9.6089	0.5707	2.3300	
				44.4319	-6.3477	2.3913	0.3331	0.0082	-0.0118		
	70ºC	1.0170	1.1764	1.7118	-16.2404	2.4023	-0.2360	10.5126	0.6317	2.6017	
				53.5637	-7.8536	3.7878	0.3963	-0.0785	0.0551		
	90ºC	-0.2236	1.2920	1.7500	-16.5851	2.4162	-0.3091	12.3600	0.7676	2.7156	
				50.0194	-7.1544	4.9556	0.3644	-0.1543	0.1009		
	All	60 parameters, 4x(9+6)									14.48%
N30	25ºC	1.4974	1.1586	1.9214	-11.3415	2.0650	-0.0081	9.0251	0.4750	2.5730	
				9.0169	-0.0062	5.9703	0.0534	-0.2697	0.0626		
	50ºC	1.7560	1.1361	1.7729	-10.6114	2.0245	0.0187	8.4019	0.4414	2.3427	
				9.4317	-0.0198	5.8196	0.0521	-0.2699	0.0374		
	70ºC	1.2924	1.1710	1.6559	-10.0414	1.9856	0.0279	7.9528	0.4220	2.1881	
				5.8642	0.5747	5.6692	0.0272	-0.2651	0.0269		
	90ºC	-0.2441	1.2987	1.4173	-9.7121	1.9530	-0.0049	7.1921	0.3948	1.9387	
				1.2653	1.3639	5.5028	-0.0061	-0.2533	0.0316		
	All	60 parameters, 4x(9+6)									9.774%
N49	25ºC	2.9209	1.0927	1.9977	-23.9579	2.8626	-0.5196	10.2641	0.5681	2.5259	
				39.7710	-5.1034	2.6720	0.2681	0.0655	0.1299		
	50ºC	2.3451	1.1476	2.1030	-25.5739	2.9597	-0.6906	10.4937	0.5804	2.6461	
				34.4150	-4.3420	1.8549	0.2420	0.1301	0.0684		
	70ºC	2.2009	1.1701	2.0792	-25.8101	2.9847	-0.7025	10.4108	0.5649	2.6640	
				38.8457	-5.0727	1.8944	0.2741	0.1390	0.0944		
	90ºC	2.2715	1.1731	1.9736	-25.4128	2.9808	-0.6315	9.8899	0.5170	2.6323	
				38.5438	-5.0093	1.8358	0.2720	0.1376	0.0884		
	All	60 parameters, 4x(9+6)									22.15%
N87	25ºC	6.1100	0.7637	1.6559	-14.7536	2.3782	0.1497	9.8501	0.5632	2.2162	
				32.9569	-4.2622	1.7386	0.2404	0.0401	-0.0725		
	50ºC	2.7582	1.0433	1.5589	-18.0318	2.5658	-0.2361	10.9395	0.6584	2.3829	
				47.1152	-6.7621	2.3148	0.3514	0.0277	0.0093		
	70ºC	1.8971	1.1157	1.6869	-17.7556	2.5284	-0.3041	11.9197	0.7292	2.5825	
				62.6670	-9.4174	3.3365	0.4664	-0.0238	0.0874		
	90ºC	0.8429	1.2119	1.8316	-17.2386	2.4832	-0.3470	13.4851	0.8385	2.8382	
				64.9932	-9.7781	4.6537	0.4829	-0.0970	0.1775		
	All	60 parameters, 4x(9+6)									13.97%

TABLE II: FITTING RESULTS FOR THE FINAL 5 MATERIALS

Mat	Temp	k_1'	a_1	b_1	k_2'	a_2	b_2	k_{rel}'	a_{rel}	b_{rel}	E_{95th}
				p00	*p10*	*p01*	*p20*	*p11*	*p02*		
Material E	25ºC	2.3859	1.1314	1.9734	-29.1130	3.2238	-0.5807	11.6155	0.6969	2.2377	
				19.6599	-1.8043	2.6016	0.1299	0.0197	-0.1340		
	50ºC	1.4351	1.2128	2.1435	-32.3441	3.4352	-0.7411	7.7280	0.3912	2.4369	
				18.0486	-1.4739	3.2517	0.1125	-0.0639	-0.3650		
	70ºC	1.7758	1.1882	2.1923	-32.5128	3.4874	-0.4860	11.4230	0.6770	2.3816	
				14.3141	-0.8358	3.6948	0.0829	-0.1775	-0.9002		
	90ºC	1.9566	1.1807	2.1885	-33.1304	3.5205	-0.5941	11.2878	0.6594	2.3600	
				36.9005	-5.1469	2.2420	0.2855	-0.0357	-0.1442		
	All	60 parameters, 4x(9+6)									23.60%
Material D	25ºC	3.5849	1.0122	1.7976	-19.0609	2.5856	-0.0737	0	0	0	
				11.3004	-0.4019	3.0320	0.0670	-0.0746	-0.1627		
	50ºC	1.2973	1.1999	1.8173	-27.8189	3.1403	-0.8648	13.3134	0.9304	1.0925	
				15.3094	-1.6607	0.9518	0.1511	0.2150	0.1075		
	70ºC	2.0268	1.1467	2.0771	-27.8331	3.1534	-0.7978	-0.2020	-0.3647	3.3655	
				-12.6105	4.3570	14.2491	-0.1631	-1.0063	-0.5620		
	90ºC	-1.9950	1.4827	2.1022	-28.7020	3.1720	-0.9693	56.7664	3.7447	5.2287	
				31.3326	-3.5993	6.4942	0.2038	-0.2248	0.0109		
	All	60 parameters, 4x(9+6)									22.87%
Material C	25ºC	-0.8090	1.2789	1.3626	-18.9273	2.6114	-0.3846	5.5581	0.3012	2.5923	
				26.7373	-3.3736	4.1984	0.2043	-0.1506	-0.0248		
	50ºC	-0.7740	1.2812	1.5520	-18.1526	2.5238	-0.4213	6.4205	0.3511	2.7855	
				41.6026	-6.0729	4.7102	0.3290	-0.1567	0.0543		
	70ºC	-0.4455	1.2615	1.8683	-18.0382	2.5584	-0.3343	5.5969	0.2720	3.0418	
				31.1284	-4.0782	7.5609	0.2357	-0.3864	0.0504		
	90ºC	-1.8676	1.3913	1.8703	-18.4802	2.5937	-0.3934	0.9339	14.0935	4.8501	
				31.4340	-4.2160	7.2207	0.2471	-0.3361	0.1190		
	All	60 parameters, 4x(9+6)									14.60%
Material B	25ºC	-0.6082	1.2897	1.8224	-12.5537	2.1550	-0.1191	5.6830	0.2541	2.9877	
				4.5861	0.3641	5.0111	0.0509	-0.1958	0.0717		
	50ºC	-0.0972	1.2595	1.8690	-11.8026	2.1140	-0.0925	3.6906	0.0925	3.0152	
				0.9186	1.0051	4.8621	0.0243	-0.1831	0.0804		
	70ºC	1.1251	1.1786	2.0075	-10.7112	2.0489	-0.0328	4.3712	0.1330	2.8837	
				-2.6573	1.7074	5.0152	-0.0087	-0.2046	0.0653		
	90ºC	-0.1711	1.2885	1.7722	-9.7093	1.9818	-0.0017	4.3702	0.1647	2.5736	
				-9.0400	2.8436	4.9328	-0.0588	-0.2100	0.0434		
	All	60 parameters, 4x(9+6)									8.074%
Material A	25ºC	4.7442	0.8548	1.4052	-18.7122	2.7643	-0.2571	2.4296	0.0808	2.4503	
				6.9005	-5.1469	2.2420	0.2855	-0.0357	-0.1442		
	50ºC	3.1228	0.9707	1.3666	-19.5150	2.8185	-0.3063	5.0173	0.2651	2.8145	
				45.3397	-6.7173	3.1549	0.3577	-0.1022	-0.1063		
	70ºC	-2.4755	1.4555	1.0968	-21.0851	2.9037	-0.5311	-5.9455	162.8406	36.2542	
				36.9005	-5.1469	2.2420	0.2855	-0.0357	-0.1442		
	90ºC	-6.8894	1.8204	1.2179	-18.4851	2.7187	-0.3902	-3.2823	106.0626	24.0666	
				35.5932	-5.4185	3.7661	0.3210	-0.0771	0.0755		
	All	60 parameters, 4x(9+6)									18.24%

For the final 5 materials, we cannot present the 95th percentiles of the validation data, but since in the original 10 materials we have seen that the errors in the model fitting dataset and the model validation dataset are very similar, we can present the fitting errors instead. Similar to TABLE I, the fitting results for the final 5 materials are shown in TABLE II.

REMARK: For the final 5 materials the code for the original 10 materials has been repurposed and executed directly without any modifications. It is very possible that the erroneous data classification from the preprocessing stage behaves differently since the final 5 datasets are composed of very different waveform type distributions, thus being a potential major source of the increased 95th percentile error compared to the original 10 materials. The relation between the 95th percentile and root mean square error appears to indicate that this is the case, since in the original 10 materials the 95th percentile is almost twice of the root mean square error, while in the final 5 materials it is up to thrice the root mean square error.

V. DISCUSSION

The model that we have presented here offers a very compact analytical approach to model core losses with close ties to the known physical phenomena governing the hysteresis, eddy, and relaxation losses. We have proven that the model is 100% generalizable between materials since it does not require any kind of fine tuning or redefinition of the loss equations depending on the material and temperature.

Since the model is built upon well-known analytical approaches [1]-[4], we hope that other works built upon th e same basis, such as the Steinmetz Premagnetization Graph presented in [5], can be intuitively integrated in the presented approach to model the behavior of other phenomena like premagnetization losses.

It is important to mention that in this work we took the approach of generating new parameters for each temperature, but looking at the parameters from TABLE I, there appear to be clear relations between the evolution of the parameters with the temperature. Looking at the k_1', it appears that it almost always decreases with temperature, meaning that the hysteresis loss plane is lowered at high temperatures. This would make sense with the physical behavior of the magnetic domains inside the material, since at higher temperatures the easier it would be for these domains to move and rotate, generating lower hysteresis losses. Thus, there is reason to believe that only one set of these material parameters could be defined for a given temperature, and that the parameters at different temperatures could potentially be obtained from modelling this behavior with the temperature. This could potentially reduce the number of parameters even further. Integrating the sinusoidal losses should not be too hard either with the well-known relation between the sinusoidal and triangular losses, thus we could reduce the number of required parameters even further.

To finish, we believe that the model proposed here would be ideal to be used as an standard kind of datasheet for material losses; it is very compact and should easily fit in a traditional datasheet, it is built upon well known literature, is tied with physical phenomena, and is really easy to implement in any software.

VI. CONCLUSION

This work represents the final report from the Mondragon university team for the MagNet challenge. The criterion behind the key decision to generate the model are justified with the aim of creating a standard approach to parametrize magnetic materials.

First, a modification of the input variables is presented, where the waveforms are transformed into simplified versions, which would be beneficial for using the model in a classical transformer design workflow. Then, the basis of the model are presented, which is built upon well known analytical approaches, combining the key concept of hysteresis and eddy loss separation, definition of losses using flux derivative and peak to peak flux density, utilization of the composite waveform hypothesis and lastly integration of the relaxation losses.

After this, the results obtained are presented, showing all the parameters used, as well as the 95th percentile errors achieved. Estimation of the results for the final 5 materials are also presented.

Lastly, a discussion is presented on why we believe that the presented model is a good candidate for material datasheets.

REFERENCES

[1] C. P. Steinmetz, "On the Law of Hysteresis," in *Transactions of the American Institute of Electrical Engineers*, vol. IX, no. 1, pp. 1-64, Jan. 1892, DOI: 10.1109/T-AIEE.1892.5570437.

[2] K. Venkatachalam, C. R. Sullivan, T. Abdallah and H. Tacca, "Accurate prediction of ferrite core loss with nonsinusoidal waveforms using only Steinmetz parameters," *2002 IEEE Workshop on Computers in Power Electronics*, 2002. Proceedings., Mayaguez, PR, USA, 2002, pp. 36-41, DOI: 10.1109/CIPE.2002.1196712.

[3] C. R. Sullivan, J. H. Harris and E. Herbert, "Core loss predictions for general PWM waveforms from a simplified set of measured data," *2010 Twenty-Fifth Annual IEEE Applied Power Electronics Conference and Exposition (APEC)*, Palm Springs, CA, USA, 2010, pp. 1048-1055, DOI: 10.1109/APEC.2010.5433375.

[4] J. Muhlethaler, J. Biela, J. W. Kolar and A. Ecklebe, "Improved Core-Loss Calculation for Magnetic Components Employed in Power Electronic Systems," in *IEEE Transactions on Power Electronics*, vol. 27, no. 2, pp. 964-973, Feb. 2012, DOI: 10.1109/TPEL.2011.2162252.

[5] J. Muhlethaler, J. Biela, J. W. Kolar and A. Ecklebe, "Core losses under DC bias condition based on Steinmetz parameters," *The 2010 International Power Electronics Conference - ECCE ASIA* -, Sapporo, Japan, 2010, pp. 2430-2437, DOI: 10.1109/IPEC.2010.5542385.

[6] A. Arruti, J. Anzola, F. J. Pérez-Cebolla, I. Aizpuru and M. Mazuela, "The Composite Improved Generalized Steinmetz Equation (ciGSE): An Accurate Model Combining the Composite Waveform Hypothesis With Classical Approaches," in *IEEE Transactions on Power Electronics*, vol. 39, no. 1, pp. 1162-1173, Jan. 2024, DOI: 10.1109/TPEL.2023.3323577.

DETAILED RESULTS FOR THE INITIAL 10 MATERIAL FITTING

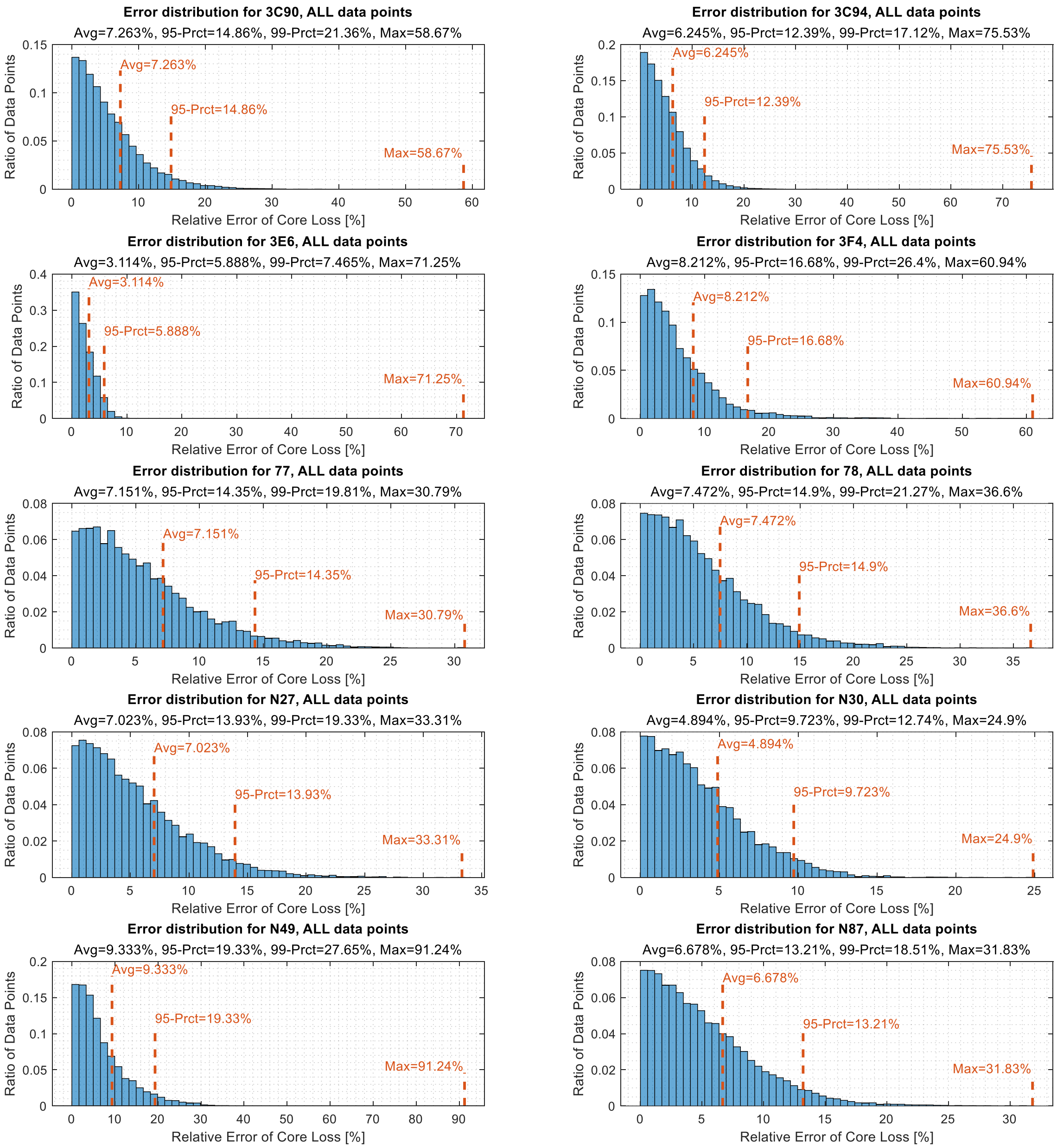

DETAILED RESULTS FOR THE INITIAL 10 MATERIAL VALIDATION

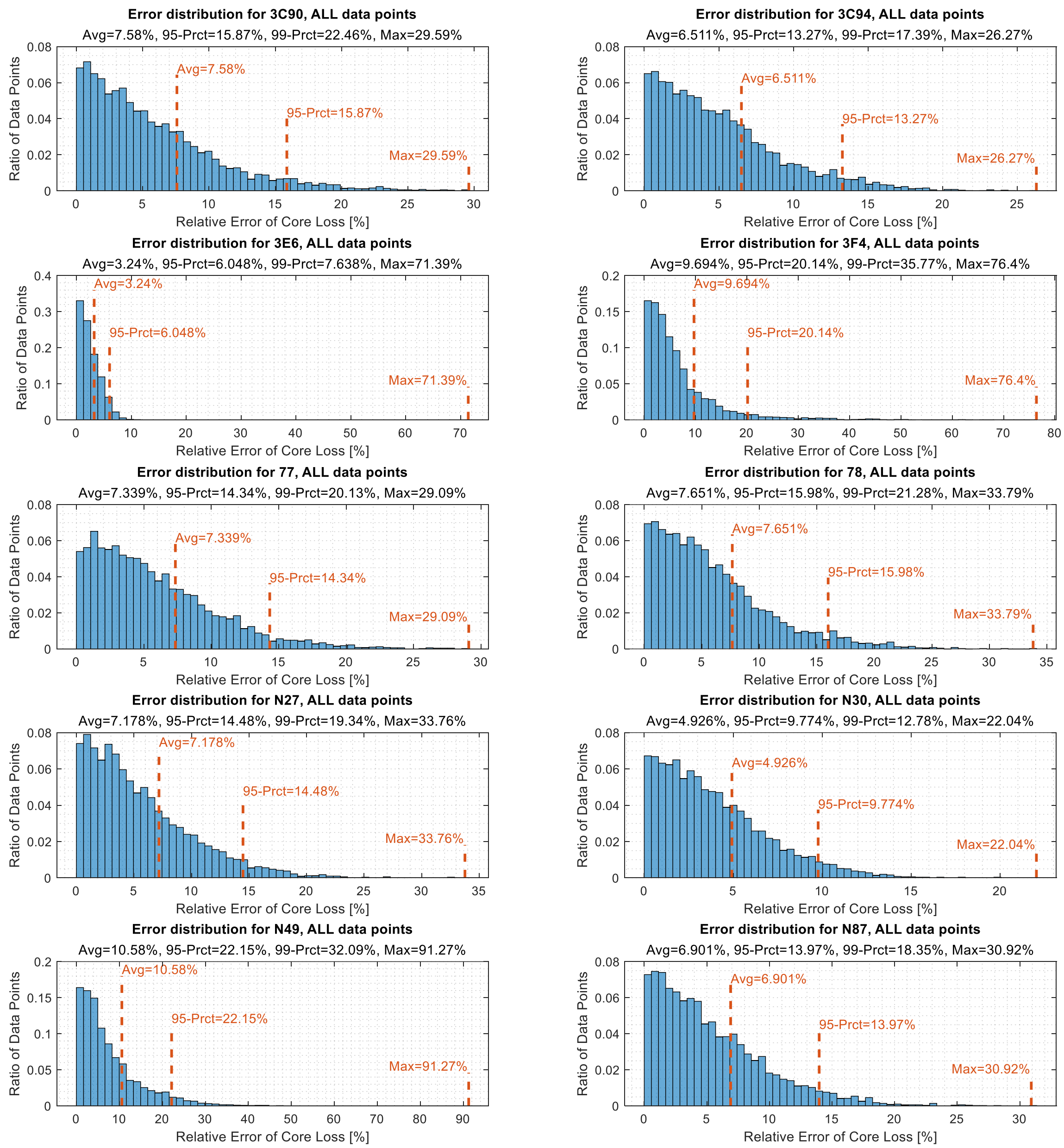

DETAILED RESULTS FOR THE FINAL 5 MATERIAL FITTING